


## Article

# Sizing of Small Hydropower Plants for Highly Variable Flows in Tropical Run-of-River Installations: A Case Study of the Sebeya River

Geoffrey Gasore <sup>1,\*</sup> , Arthur Santos <sup>2</sup> , Etienne Ntagwirumugara <sup>1</sup> and Daniel Zimmerle <sup>2</sup>

<sup>1</sup> African Center of Excellence in Energy for Sustainable Development, University of Rwanda, Avenue de l' Armée, Kigali P.O. Box 3900, Rwanda

<sup>2</sup> Energy Institute, Colorado State University, 430 N. College Avenue, Fort Collins, CO 80524, USA

\* Correspondence: g.gasore@ur.ac.rw; Tel.: +250-7865-85881

**Abstract:** Rivers in tropical climates are characterized by highly variable flows which are becoming more variable due to climate change. In tropical conditions, most hydropower plants are designed as run-of-river plants with limited water storage. The aim of this study is the selection and sizing of a hydropower plant for highly variable flows, using the Sebeya River as a case study. As is often the case, flow data was incomplete, and the study also demonstrated the use of machine learning to predict the Sebeya flow rate for 2019. Stochastic modeling was used to estimate the energy generation for multiple turbine types and the levelized cost of energy for all configurations, capturing the uncertainty in many of the input parameters. River flow varies between 1.3 m<sup>3</sup>/s and 5.5 m<sup>3</sup>/s in a year; the minimum LCOE occurs at the knee in the flow exceedance curve of river flow rate, near 1.8 m<sup>3</sup>/s. The optimal LCOE for the Sebeya river is around 0.08 \$/kWh with an uncertainty of −0.011/+0.009 \$/kWh. Additionally, certain turbine types—notably propeller turbines—perform poorly in this type of highly variable flow. The method and findings can be used to guide future investments in small- to mid-sized hydropower plants in similar climatic conditions.

**Keywords:** small hydropower; variable river flow; renewable energy; tropical energy projects; stochastic modeling



**Citation:** Gasore, G.; Santos, A.; Ntagwirumugara, E.; Zimmerle, D. Sizing of Small Hydropower Plants for Highly Variable Flows in Tropical Run-of-River Installations: A Case Study of the Sebeya River. *Energies* **2023**, *16*, 1304. <https://doi.org/10.3390/en16031304>

Academic Editors: Helena M. Ramos and Matteo Postacchini

Received: 26 August 2022

Revised: 29 December 2022

Accepted: 3 January 2023

Published: 26 January 2023



**Copyright:** © 2023 by the authors. Licensee MDPI, Basel, Switzerland. This article is an open access article distributed under the terms and conditions of the Creative Commons Attribution (CC BY) license (<https://creativecommons.org/licenses/by/4.0/>).

## 1. Introduction

There is an increasing need for reliable technical information to inform or act as a reference for investors in hydropower development in tropical run-off rivers especially in developing countries where there is a scarcity of time series data on river flow rates and a lack of published feasibility studies on plants. Hydropower is a widely deployed renewable energy technology, reliable, and in most cases, considered an inexpensive renewable energy source, with a levelized cost of electricity (LCOE) ranging from 0.05–0.10 US \$/kWh [1]. This is reinforced by prior analyses (Panwar et al.; 2011; Chu and Majumdar, 2012; Jiang et al., 2018, as cited in [2] indicating that hydropower is an affordable, reliable and the most deployed renewable energy technology.

Renewable energy are energy sources which are refilled at a higher rate compared to the rate of consumption and produce lower emissions in comparison to fossil fuels. Examples of renewable energy are solar energy, wind energy, geothermal energy, hydropower, ocean energy and bioenergy [3].

In Africa, hydropower is the most developed renewable energy source, with a total installed capacity of 53 GW or approximately 63% of the total deployed renewable energy. However, Africa needs additional generation as a catalyst for economic development, while simultaneously controlling greenhouse emissions. As of this writing, the continent has developed only 11% of its hydropower potential [4].

Hydropower plants are classified based on different factors such as water inflow regulation available, size of installed plant capacity, and type of load being supplied. Regarding water inflow regulation, hydropower power plants are classified into three categories: (1) Reservoir plants, which have a dam and reservoir that stores water and regulates water inflow; (2) “Run-of-river” (RoR) plants, which have minimal reservoir capacity—typically a small diversion dam and catchment—and the water supply is mainly determined by the current river flow; and (3) pumped storage plants, which have both upper and lower reservoirs. During low-power demand, pumped storage uses electricity to pump water from the lower to the upper reservoir, and uses water from the upper reservoir for electricity generation during high demand [1].

Hydropower power can also be classified as large or small depending on the plant’s generation capacity. Small hydropower plants have a generation capacity up to 10 MW but specific definitions vary between countries [5]. There are three other commonly accepted classes of hydropower plants: mini (100–1000 kW), micro (10–100 kW) and pico (<10 kW). Plants of these sizes are sometimes classified independently or included in the small hydropower plant category.

In Rwanda, the total installed capacity, by rated power, for all energy sources is 238 MW, of which renewable energy accounts for 55%. Total capacity, in descending order is: 44% hydropower, 25% thermal (primarily marine diesel), 8% methane gas (harvested from Lake Kivu), 8% imported and shared resources with neighboring countries, 6% peat-fired thermal plants and 5% solar photovoltaic [6]. Small-scale hydropower includes 44 plants [6], all of which are RoR. The country is characterized by a tropical climate with dry season river flows that are 50% or less than wet season flows [7]. Rwanda is commonly characterized as having four seasons: A short rainy season (from September to November), a long rainy season (between March to May), a short dry season (between December to February) and a long dry season (from June to August). Recent climatic data indicates that rainy seasons are becoming shorter but with higher intensity rainfall events [8]. This change is likely to increase the variability in river flows [9].

Sebeya River is located in the western part of Rwanda and is the largest catchment in the region. The Sebeya originates in high elevation mountains along the edge of Nile–Congo divide in the Rutsiro District. The river runs through Gishwati national park and discharges into lake Kivu with a length of 110 km [10]. The whole region of East-Central Africa has experienced an average temperature increase of 0.29 °C from 1985 to 2015, and Rwanda in particular has experienced large fluctuations in annual rainfall over the 55-year period from 1961 to 2016 [11].

The plants which are the focus of this study—small RoR hydropower plants—have minimal reservoir capacity and use immediate river flows for electricity generation [1]. As a result, these plants are sensitive to seasonal weather variations that impact river flow. In particular, this study deals with sizing a hydropower plant in these highly variable flow conditions, proposing a methodology for analysis and suggests general conclusions on the optimal design flow rate and turbine type for cost-effective electricity generation. This analysis is of interest to future investors in the run-of-river hydropower plants in similar climatic conditions.

Hydro turbines are classified into two types: impulse and reaction turbines. In reaction turbines, water flows over runner blades and energy production results from the pressure caused by changes in direction of the moving water. Reaction turbine types include Francis, Kaplan and propeller turbines. In impulse turbines runner buckets redirect a jet of water impacting a runner’s curved buckets, creating a change in momentum and resulting force [12]. Impulse turbine types include Pelton, crossflow and Turgo turbines.

In turbine selection, there is a set of requirements and specifications which include either site conditions (head and flow rate) and/or output power requirements [13]. In general, turbine selection is based on the available head and flow conditions in comparison to standard charts during initial sizing, while detailed design includes additional analysis to consider technical, social, environmental, and economic factors [14]. The work performed

here is focused on the initial design phase, when a developer is primarily interested in the initial sizing to estimate the cost of civil works, permitting, land-access costs, and similar preparatory steps, prior to detailed design.

The previous literature identified several technical parameters considered in the sizing of hydropower plants and predicting energy generation. In the design process, sizing of a hydropower plant size is primarily determined by head, reservoir size, minimum downstream flow rate, and river seasonal inflow [11]. A study by Fairuz et al. [15] on factors affecting mini hydropower production efficiency concluded that humidity and rainfall have a significant effect on the power generation in mini hydropower plants and can be used to predict energy generation. A study by Singh et al. [16] concluded that head, discharge, and generator parameters affect the operation of RoR hydropower plants. A study by Aggidis et al. [17] on the costs of small-scale hydropower production concluded that the cost of manufacturing mini hydropower turbines is determined by the hydraulic characteristics of the hydro resource available and changes with turbine size and type.

It also defined the levelized cost of electricity (LCOE) and identified parameters considered in computing LCOE of different renewable energy technologies. LCOE is a measure used in estimating the cost of generating electricity over a lifetime of any generation technology. It can also be used to determine the cost-effectiveness of electricity generation of any technology without taking in account the assumptions of price at which generated electricity is sold to both the end user and the grid. Again, from the LCOE one can determine whether a technology is profitable or not. If the LCOE is lower than the price at which the generated electricity is sold, it is profitable and when the LCOE is greater than the price at which the generated electricity is sold it is unprofitable [18]. Different studies have identified different important parameters to be considered in calculating the LCOE of different technologies. A study by Patro et al. [19] on clean development projects in India found that in recent years many developers of small hydropower plants conduct life cycle costing studies without ignoring any costs which were used before operating and maintaining the plant, replacement, certified emission and others. A review of the LCOE of solar photovoltaics by Branker et al. [20] on how to get the correct LCOE of solar photovoltaics concluded that due to the highly variable LCOE inputs of solar technology, to get correct LCOE outcome, almost all costs associated with solar electricity generation should be included. A study by Ouyang et al. [21] on the LCOE of renewable energies and required subsidies in China found the accurate cost estimations of renewable energies were urgently needed to accelerate renewable energy development. The study recommended that the existing feed-in-tariff (FIT) be improved and adjusted based on the LCOE and to provide subsidies in the short-term to reduce the high-cost of renewable energy.

Additionally, previous work has identified that low-quality pre- and full-feasibility studies contributed to project failure [22], and a study by Fairuz recommended the use of machine learning to improve predictions of energy generation [15]. In Rwanda, there is no similar published work, and, unfortunately, there is little time series data for river flow (discharge rates). Therefore, to systematically size mini-hydropower plants for Rwandan rivers, such as the Sebeya, it is necessary to both estimate the river flows and to use those flows to estimate the optimal sizing of the power plant. Thus, the Sebeya flows were predicted using a neural network (scaled conjugate gradient or SGC method) by inputting both secondary data (using precipitation and flow rate) and primary data (collected flow rate at the Sebeya river).

## 2. Materials and Methods

### 2.1. Flow Rate Estimation

To size a small RoR hydropower plant for any river, a time series flow rate of the river is needed. However, the only available historical consistent flow rate of the Sebeya from a Rwanda Water Resource Board was from 2017. By 2019, historical flow rate data was inconsistent or missing for the Sebeya river. There the report from 2017 was the best method for predicting, given that the lack of data is a real issue for other sites. Machine learning

is being used in different approaches to help forecast energy generation, and improve the operation, design, and maintenance of hydropower plants. Among other applications, it has been implemented in the optimal dispatch of hydropower plants based on head and river flow [23], to assess hydropower reliability due to climate change [24,25], reservoir water level forecasts [26], and to help mitigate silt erosion in the hydro-mechanical components of the plant [27]. Yang et al. used a deep learning method to predict hydropower generation at small plants based on historical precipitation data provided by weather stations with 93% accuracy, [28]. However, access to reliable and consistent data often remains a challenge in such studies [29]. This study used the Sebeya 2019 precipitation from the Rwanda Meteorology Agency, available Sebeya flow rates from 2017 (provided by the Rwanda Water Resources Board) since there were no historical consistent flow rates of the Sebeya for 2019, and Sebeya field visit measurements conducted in 2019 (19 April 2019, 17 May 2019, 29 June 2019 and 20 August 2019). Using these data, machine learning was used to predict the Sebeya flow for the observed weather conditions in 2019, a timeframe where near-continuous meteorological data was available for the watershed area of the river. The methodology used is shown in Figure 1.

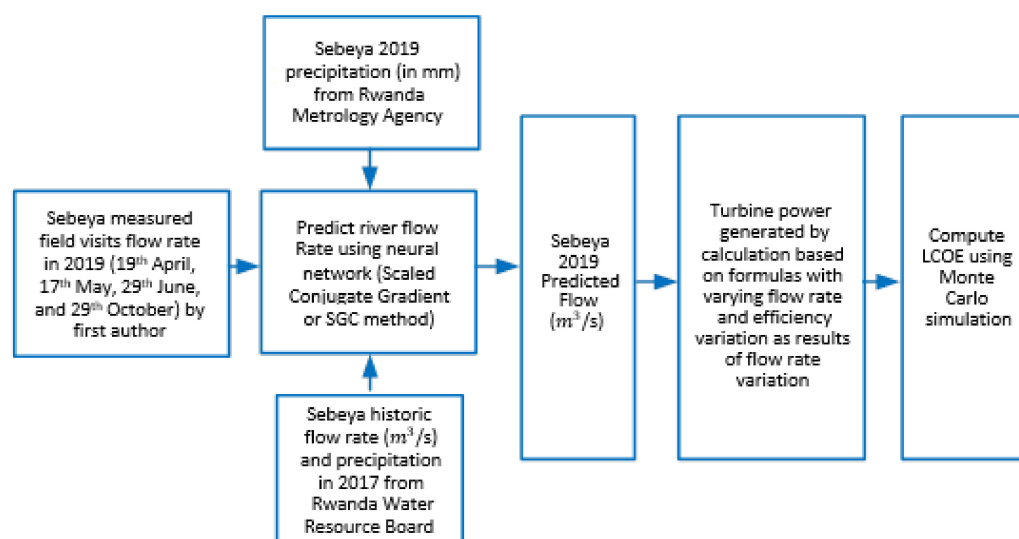


**Figure 1.** Methodology for estimating river flow rates.

The machine learning method estimated river flow data for 2019, using daily precipitation in the Sebeya river watershed during 2019 after being trained on the available Sebeya flow rate data from 1 May 2017 to 31 December 2017. The training data represented the longest period of near-continuous flow rate data available—200 days of data, spanning wet and dry seasons, with coincident records for both precipitation and river flow. In contrast, only precipitation was available for 2019, the year when the study was conducted. Therefore, data from 2017 was utilized to train a neural network (NNET), and the trained model took as its input precipitation, and predicted the river flow.

Training used the scaled conjugate gradient (SCG) method. SCG is a supervised learning algorithm that minimizes the error between its results and a target variable, using a defined error function [30]. The advantage of this method in comparison with others, like Adam and scaled gradient descent, is that it does not need a learning rate and therefore is less dependent on user inputs, making it effective for large-scale problems [31].

According to the US Geological Survey [32] and US rivers, basin lag time—the difference between peak rainfall and peak discharge of the river—varies from 0–105 h. To accommodate this lag, the model uses the 10 previous days of precipitation, approximately two times the estimated basin lag time.

The Sebeya river flows are characterized by high flow rate events shortly after heavy rain in the watershed of the river. Therefore, special precautions were taken to assure that

predicted river flow rates—in practice, 1000 Monte Carlo iterations of the model—reflected the nature and magnitude of these events.

First, error was calculated using mean absolute error (MAE), rather than root mean squared error, as MAE assigns less weight to the large errors. This allows the fitted model to better retain points that deviated substantially from the norm, i.e., to better model high rainfall events. Figure 2 provides an example. The middle plot compares the training data to the predicted data for one iteration of the model. From index 25 to 80, the river flow is nearly constant as this is the dry season, with few rainfall events. Later indices indicate the start of the rainy season, characterized by periodic rain events and a higher variation in river flow rate.

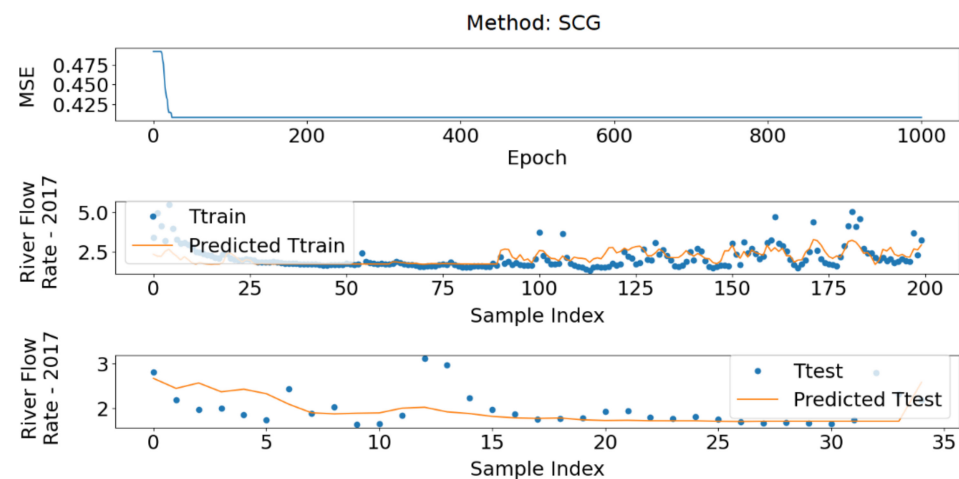


**Figure 2.** Machine learning results. The upper panel shows the error function over the training generations, the middle panel compares the predicted output with the training data, and the lower panel tests data with the predicted data.

The training and error functions were selected to retain the extreme flow events, which are observed on the river following major rainstorms. One example of a predicted river flow rate is shown for 2019 in Figure 3.

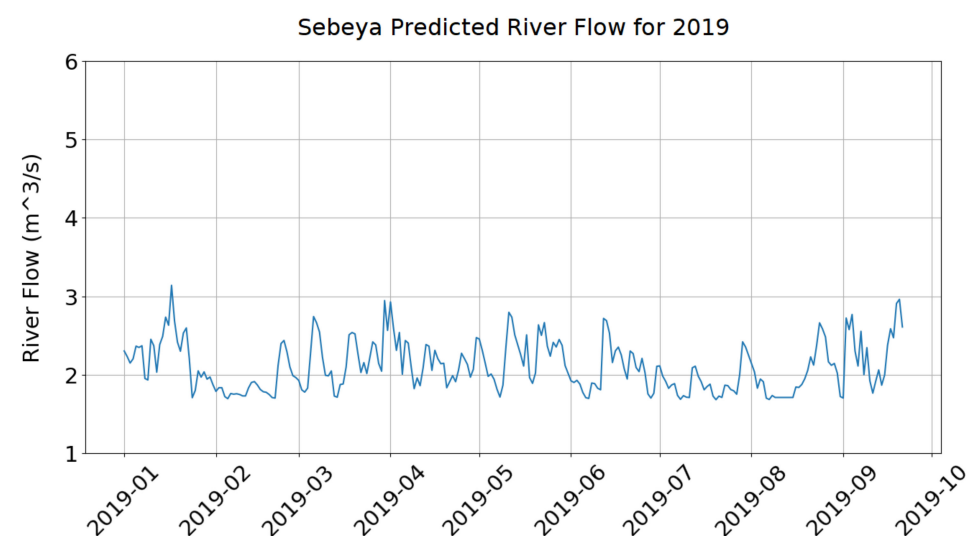


**Figure 3.** River flow prediction for 2019, prior to capturing high flow events.

From Figure 2, during the period with high variability in the rainy season river flow (index 80 onwards), the model output does not capture high variations in the river flow seen in the training data, i.e., from actual flow measurements. This is characteristic of

machine learning models for this type of application. To add this high variability back into the model results, the predicted flow was adjusted by adding in the deviation between the neural network (NNET) prediction and the training data observations of the actual flow. The method used was as follows: NNET outputs were binned at  $0.1 \text{ m}^3/\text{s}$  intervals; an error distribution between the NNET prediction and the training data was calculated for each bin; the NNET prediction for 2019 was adjusted by randomly adding a deviation drawn from the error distribution of the correspondent NNET bin. Adding these adjustments further restores extreme river flow events to the smoothed NNET results.

Each run of the trained NNET results in a different prediction of the river flow rate. This process was performed 1000 times, creating a family of 1000 plausible daily average river flow rate predictions for the Sebeya in 2019, see Figure 4.

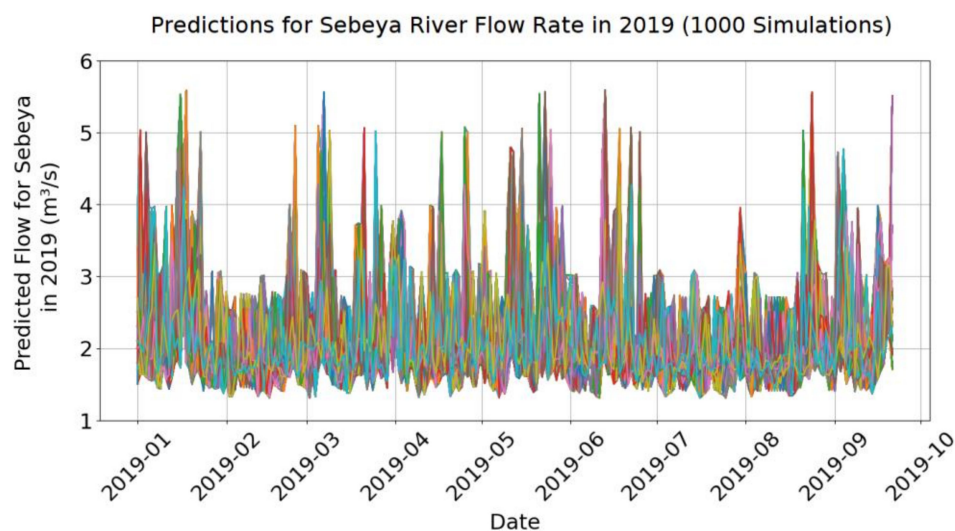


**Figure 4.** Adjusted predictions for the Sebeya river flow in 2019. In the chart, each of the one thousand simulations performed is represented by a line in a different color. All 1000 iterations are overlaid in the figure. Vertical width on any time step illustrates the randomized range of the river flow rate for each time step.

As noted earlier, limited river flow rate data was available, and the data available had substantial periods with no, or suspect, flow readings. Therefore, to provide a limited 'spot check' of the model, the first author measured the river flow at a power plant located on the river on four dates: 19 April 2019, 17 May 2019, 29 June 2019, and 20 August 2019, resulting in measurements of  $4.24 \text{ m}^3/\text{s}$ ,  $3.3 \text{ m}^3/\text{s}$ ,  $1.96 \text{ m}^3/\text{s}$ ,  $1.61 \text{ m}^3/\text{s}$ , respectively. A simple measurement process was performed: Timing the movement of a float on the surface of the river, measuring the cross-sectional depth of the river, and applying appropriate hydraulic calculations. We compared these data to the distribution of results for the measurement days, as shown in Figure 5.

Two measurements were well within the inner quartile of the predicted flows, while the other two measurements were within the outer quartile and within the range of the outlier data, respectively. It should be noted that Rwanda was in drought conditions in 2017, while 2019 was considered a rainy year. While limited in scope, these measurements indicate that the model produces values, including outliers, which are representative of the observed conditions.

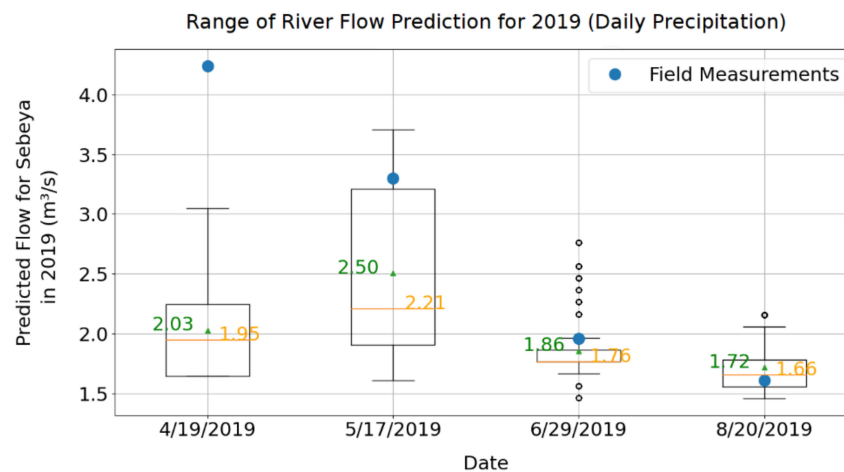


**Figure 5.** Predicted and measured river flow rate. Boxplots represent the inner and outer quartiles and outliers. Blue points are measured river flow rates.

## 2.2. Power Production Estimation

The analysis utilized here develops a first-order simulation of the turbine performance, using the 1000 Monte Carlo iterations predicting the river flow rate.

Turbine produced power, is:

$$P_w = \frac{1000 * 9.81 * q_d * h}{1000} = 9.81 * q_d * h \quad (1)$$

$$P = \eta_m \rho q_d g h \quad (2)$$

where  $g$  is the acceleration of gravity ( $m^3/s$ ),  $q_d$  is the flow rate of the river in  $m^3/s$  used to select the turbine and design the power plant ('designed flow rate'),  $h$  is the working head of the river net of friction losses in the penstock and head gates ( $m$ ),  $\eta_m$  is the efficiency of the turbine at the designed flow rate, and  $\rho$  is the water density  $\frac{1000 \text{ kg}}{m^3}$ . For this study, we assumed the plant was designed such that the efficiency is maximized at the designed flow rate, i.e.,  $\eta_m$  is the maximum efficiency of the turbine, typically at or near full load.

For the Sebeya River, the flow rate ( $q_d$ ) varies between  $1.3 \text{ m}^3/s$  and  $5.5 \text{ m}^3/s$  under non-flood conditions. In this study all plants were designed for flows below  $3.5 \text{ m}^3/s$ . Water above this flow rate would be directed around the turbine via spillway gates and not contribute to power production.

For conditions away from the designed flow rate, Equation (1) can be considered as a general function of the river flow rate and efficiency, since all other parameters remain fixed after the plant is designed. Further, efficiency is also a function of the deviation of the current flow rate from the designed flow rate, resulting in:

$$P = \mathcal{F}(q, \eta) = \mathcal{F}(q, \mathcal{G}(q)) \quad (3)$$

where  $\mathcal{F}$  and  $\mathcal{G}$  are arbitrary, typically discretized functions of flow rate. Flow rate  $q$  is determined by the analysis in the previous section for all times considered in the study, and, in general,  $\eta = \mathcal{G}(q)$  is the result of empirical testing of the selected turbine; see below. In practice the analysis utilizes normalized calculation throughputs, where performance of the hydropower plant is expressed as fractional power output calculated at the given flow rate, relative to the designed flow rate. Fractional flow rate is:

$$F_q = \frac{q_p}{q_d} * 100 \quad (4)$$

where  $F_q$  is the fraction of designed flow, in percent,  $q_d$  is the designed flow rate, and  $q_p$  is the predicted flow rate of the river.

Turbine efficiency for each turbine type was estimated by digitizing a generic turbine efficiency chart [33] that provided the efficiency at flow rates relative to the designed flow rate of the turbine. Data is valid from 5–100% of the designed flow rate, and digitization was conducted at an interval of 5%, see Figure 6.

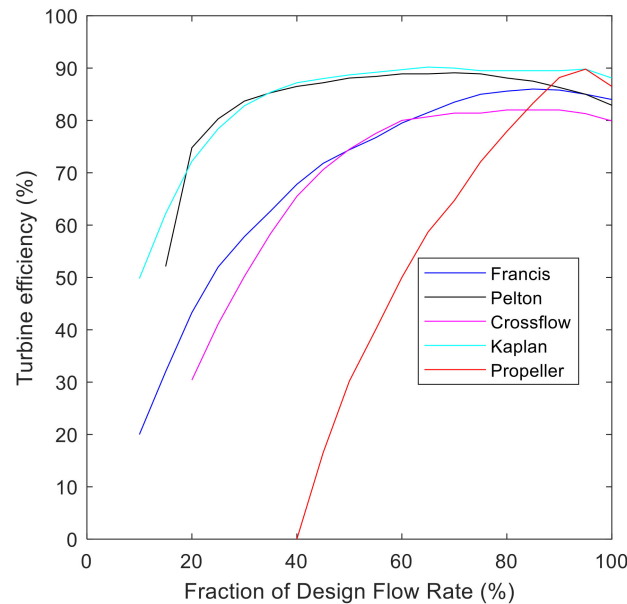


**Figure 6.** Summary plot of the turbine efficiencies relative to the designed flow rate.

Energy produced per turbine type was constrained to 100% of the designed flow rate, resulting in:

$$E_i = \begin{cases} F_{qi} & q \leq q_d \\ 100 & q > q_d \end{cases} * \eta_i \Delta t \quad (5)$$

where  $E_i$  is energy produced relative to the designed conditions during one time step  $i$ ,  $\Delta t$  is the time step of the simulation—1 day in this analysis—and  $F_q$  and  $\eta$  are calculated for each time step. Using the predicted flow rate, turbine net efficiency for the simulated time period is:

$$N_e = \frac{1}{n} \sum_{i=1}^n E_i \quad (6)$$

where  $N_e$  is the net turbine efficiency relative to the power produced, across all Monte Carlo simulations, for a given turbine, sized for a selected designed flow rate. The number of periods used to simulate  $N_e$ ,  $n$ , is the product of the length of the simulated river flow (262 days) and the number of Monte Carlo iterations, 1000. The designed flow rate of the powerplant,  $q_d$ , was simulated for 1 m<sup>3</sup>/s to 3.5 m<sup>3</sup>/s. In practice, any duration of river flow rates, at any available time step, could be substituted providing peak and trough flow events, and are statistically represented in the simulation.

To compute the total energy produced for the purpose of computing the levelized cost of energy (LCOE), power in the water at the designed flow rate, as per Equation (1), is multiplied by net efficiency,  $N_e$ , and annualized to one year:

$$E_t = 8760 P_w N_e \quad (7)$$

where  $E_t$  is the electricity generated in one simulated year.



### 2.3. Levelized Cost of Electricity (LCOE) Generated

A simplified cost model was utilized for plant sizing and costs, to provide general information on the tradeoffs between plant sizes, as is appropriate for the early planning stages simulated here.

The head is assumed for reasonable locations on the Sebeya river, and the type of turbine being used; a typical maximum gross head is 80 m. Costs can be broken into two components. The first component is an up-front investment in non-reoccurring engineering costs, permitting, legal fees, loan applications and processing fees, supervision cost, studies, etc. This value is uncertain, but for practical implementations in Rwanda, a reasonable range is between 250,000–500,000 USD for a small hydropower plant. Lacking any information about the distribution of these costs, we assumed uniform distribution.

The second component scales with the size of the plant. Using confidential data from two hydropower developers operating in Rwanda, the study assumed a required investment uniformly distributed between 2500–3000/kW USD. Using the renewable energy technologies cost analysis series report [34] and estimates from hydropower owners in Rwanda, the study assumed the operation and maintenance (OM) cost per \$ capital cost uniformly distributed between 0.025–0.03 \$/\$ capital investment.

To assume plant operating uptime and lifetime, owners of existing power plants were asked to estimate both parameters; resulting in an operating uptime of 0.85 and a plant design life of 18 years. Similarly, to assume a discounted rate, several banks in Rwanda were interviewed, resulting in a discounted rate of 12%.

Given the above assumptions, the LCOE for renewable energy is calculated as;

$$\text{LCOE} = \frac{\sum_{t=1}^{n_t} \frac{I_t + M_t + F_t}{(1+r)^t}}{\sum_{t=1}^{n_t} \frac{E_t}{(1+r)^t}} \quad (8)$$

where LCOE is the average levelized cost of electricity generated,  $I_t$  is investment expenditures in the year  $t$ ,  $M_t$  is operation and maintenance expenditures in the year  $t$ ,  $F_t$  is fuel expenditures in the year  $t$ ,  $E_t$  is the electricity generated in year  $t$ ,  $r$  is the discount and  $n_t$  is the economic life of the system.

### 2.4. Return on Investment (ROI)

Return on investors is a measure of business project profitability.

$$\text{ROI} = \frac{N_g}{C_i} * 100 \quad (9)$$

where ROI is the return on investment,  $N_g$  is net gain and  $C_i$  is cost of investment. From return on investors, one can tell whether a business project is profitable or not [35]. A positive return on an investment means a profitable business while a negative return on an investment means an unprofitable business.

## 3. Results

### 3.1. Best Turbine Type and Designed Flow Rate at Sebeya

The primary metric of interest to evaluate the design of the plant is the capacity factor, defined as:

$$\text{CF} = \frac{24 * N_e * E_t}{E_t * 8760} = \frac{N_e}{365} \quad (10)$$

where CF, the plant capacity factor, is the ratio of actual energy generated by the plant to the maximum energy that could be generated by the plant working at full capacity over a period of time.

Energy generated by the plant per year (kWh/year) is mainly influenced by the available river flow rate over a year. Variation in the river flow rate affects turbine efficiency for multiple turbines as reflected in the turbine efficiency chart [12] and Equation (3). A

designed flow rate with the highest capacity factor for any given turbine type harvests the maximum power from the water flow, given the characteristics of the river.

Capacity factor simulation results in Figure 7 indicates that Francis, Kaplan, Pelton and crossflow turbines operate across a wide range of flow rates at relatively high-capacity factors, while the capacity factor of propeller turbines is only near maximum over a narrow range of flow rates. This drop-off in efficiency of propeller turbines typically makes them unsuitable for the highly variable flows in tropical RoR plants. Therefore, this type of turbine is not considered further in this study.

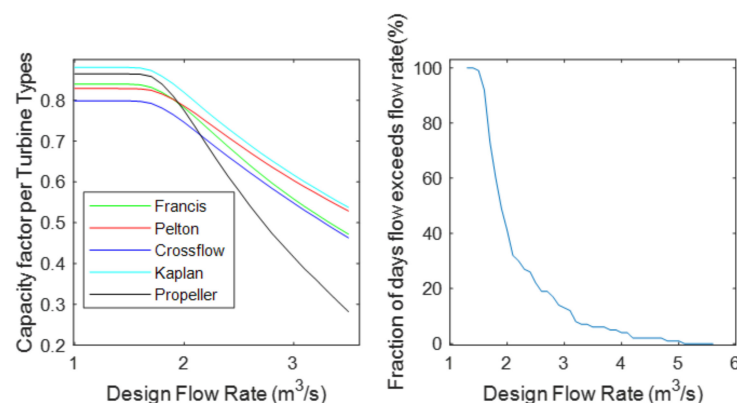


**Figure 7.** Capacity factor as a function of the river flow rate. Left panel: plant capacity factor for several common turbine types, as a function of the designed flow rate of the hydropower plant. Right panel: River flow exceedance curve.

It is also observed that the capacity factor for all the turbines is flat up to  $1.7 \text{ m}^3/\text{s}$  because there is an increasing power in the water flow at near-constant turbine net efficiency, which maintains the power produced at the designed power plant capacity. In contrast, the capacity factor drops at designed flow rates above  $1.7 \text{ m}^3/\text{s}$  as the number of days with available water at the designed flow rate drops off rapidly above  $1.7 \text{ m}^3/\text{s}$ —as shown by the right panel in the figure—and the plant is operating below the designed capacity, and at reduced efficiency, for an increasing number of days per year as the designed flow rate increases. As can be seen from the figure, the drop in the capacity factor is closely aligned with the knee in the flow exceedance curve. Therefore, it is reasonable to expect the optimal LCOE at or near that flow range.

Given the tight grouping of the capacity factor curves, for subsequent analysis, the study focused on the most commonly utilized impulse turbine type (Pelton), and one type of reaction turbine commonly utilized in small hydropower applications (Francis). Other turbine types were calculated but are not shown here for clarity.

### 3.2. Calculation of Annual Energy Produce (kWh) Per Turbine Type

From Equation (3), the power generated is a function of the designed flow rate and turbine efficiency, which is dependent on the turbine type [33]. This variation in turbine efficiency will affect the total power generated as per Equation (7).

From Figure 8, for both turbines the annual average energy produced from the designed flows of  $1.7 \text{ m}^3/\text{s}$  to  $2.9 \text{ m}^3/\text{s}$  increases monotonically as a result of the increasing water flow rate at similar high-operating efficiencies. Above a designed flow of  $2.9 \text{ m}^3/\text{s}$ , the annual average energy produced by the Francis flattens and then decreases as the increased power in the water flow cannot make up for the decreased turbine efficiency—the turbine is operating below its designed flow rate for substantial fraction of the year. The Pelton turbine, in contrast, continues to increase as it has a flatter efficiency curve resulting in a flatter power production.

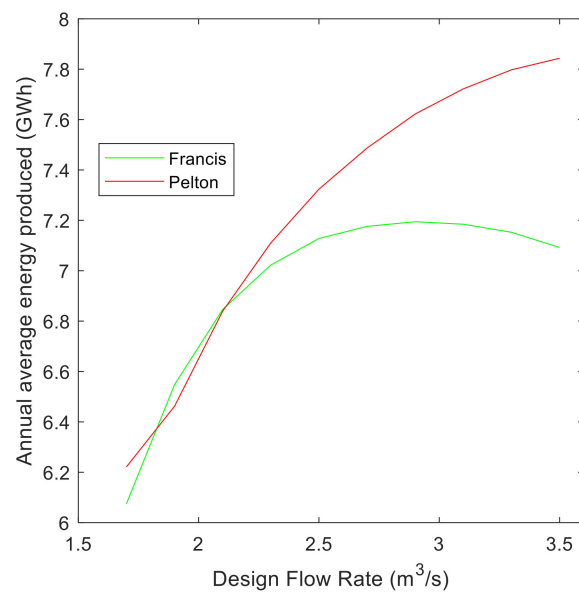


**Figure 8.** Annual average energy produced (GWh) at varying designed flow rates at a constant head of 70 m for the Francis and Pelton turbines.

### 3.3. Plant LCOE for the Francis and Pelton Turbine Performance at a Constant Head and Varying Designed Flow Rate

Different turbine types perform better in different head ranges, Pelton performs better in the high head range ( $h = 100$  m), Crossflow and Francis perform better in the medium head range ( $30 \text{ m} < h < 100$  m), while Kaplan perform better in the low head range ( $h < 30$ ). Figure 9 shows the LCOE curves of Francis and Pelton at a constant head and varying river flow rate. The LCOE sets the acceptable contract price for generated electricity in most power purchase agreements.

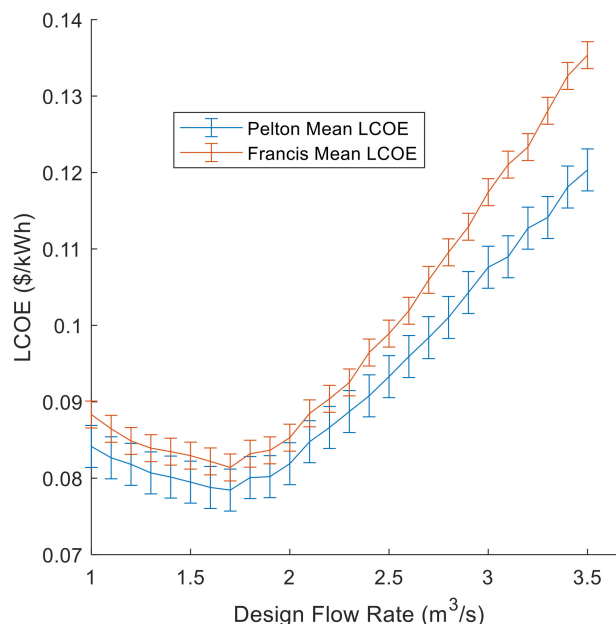


**Figure 9.** The LCOE (\$/kWh) for Francis and Pelton at varying designed flow rate (m<sup>3</sup>/s) and a constant head of 70 m. Error bars indicate 95% confidence intervals for each simulated LCOE point.

From Figure 9 and Table 1, including uncertainty, the range of the equivalent minimum LCOE, accounting for uncertainty, occurs near the knee in the flow exceedance curve, indicating that the capacity factor has the dominant influence on the LCOE, overwhelm-

ing the other factors simulated in this analysis. Given the current electrical pricing in Rwanda, plants designed at the minimum LCOE would likely be cost effective, although power purchase agreements should be negotiated to include the downside uncertainty—approximately \$0.01 \$US/kWh.

**Table 1.** The Francis and Pelton minimum LCOE and range of the equivalent minimum LCOE including uncertainty at a net head of 70 m.

Turbine Type	Minimum LCOE (\$/kwh) Including Uncertainty		Designed Flow Rate (m <sup>3</sup> /s) that Produced the Minimum Cost
	Minimum LCOE	Uncertainty	
Francis	0.082	−0.011/+0.009	1.6 and 1.7
Pelton	0.082	−0.011/+0.009	1.6, 1.7 and 1.8

Return on investment (ROI) for plant with Francis turbine

$$\text{ROI} = \frac{(\text{Price of selling electricity to grid}(\$/\text{kwh}) * \text{Average operating load}) - \text{LCOE} * \text{plant size}}{\text{LCOE} * \text{plant size}} * 100$$

$$\text{ROI} = \frac{(0.1205 * 1023) - 0.082 * 1442}{0.082 * 1442} * 100 = 4.252\%$$

#### 4. Conclusions

This study illustrates a methodology for analyzing RoR hydropower plants in a tropical climate where rivers are characterized by highly variable flows, which are undocumented or poorly documented. This method allows for the analysis of RoR plants by using realistic flow distributions, rather than relying on reservoir assumptions that smooth river flow rates or single-point estimates based upon assumed ‘average flows’. Indeed, assuming average flow—a common reservoir assumption—will often over-size a small hydropower plant, producing an unexpectedly high LCOE in operational conditions. Additionally, an oversized plant may wear more quickly than one that is properly size, an issue often seen in the field in Rwanda.

The study found that a relatively simple neural network model, trained across two complete hydrological seasons, produced a similar flow behavior to the available river flow rate measurements. While not ideal, this type of extrapolation is valuable for early planning decisions, when flow data is not available, and common average flow assumptions are not valid for RoR plants.

Finally, using a Monte Carlo analysis approach provides a template to capture the uncertainty in inputs for first-order analyses of small power plants. The approach requires reasonable up-front engineering effort and easily captures variability in values for many key variables. The LCOE results coupled with the uncertainty estimates provides the analyst with both a specific target LCOE for decision-making, and guidance on the confidence to place in that number.

Finally, absent any similar analyses, investors are advised to design RoR plants at, or just below, the ‘knee’ in the flow exceedance curve. The Sebeya river is typical of tropical conditions, and plants designed substantially above that knee produced a significantly higher LCOE. This observation also illustrates that time series of daily river flow—and corrections to those flows for expected withdrawals over the life of the plant—are a critical input to investment decisions. Jurisdictions interested in small hydropower development are therefore encouraged to invest in river monitoring as a catalyst to development.

**Author Contributions:** G.G., took the lead in all aspects of the study and writing while the other authors contributed to the following: Conceptualization, D.Z.; methodology, D.Z. and A.S.; writing—review and editing; D.Z. and E.N., writing—original draft; D.Z. All authors have read and agreed to the published version of the manuscript.

**Funding:** This research received no external funding.

**Data Availability Statement:** Apart from field data collection, the rest of data used in simulation were provided by Rwanda water resources board and Rwanda meteorology Agency.

**Conflicts of Interest:** The authors declare no conflict of interest.

## References

1. International Finance Corporation. Hydroelectric Power: A Guide for Developers and Investors. 2012. Available online: [https://www.ifc.org/wps/wcm/connect/topics\\_ext\\_content/ifc\\_external\\_corporate\\_site/sustainability-at-ifc/publications/hydroelectric\\_power\\_a\\_guide\\_for\\_developers\\_and\\_investors](https://www.ifc.org/wps/wcm/connect/topics_ext_content/ifc_external_corporate_site/sustainability-at-ifc/publications/hydroelectric_power_a_guide_for_developers_and_investors) (accessed on 4 July 2022).
2. Wei, L.; Jiheng, L.; Junhong, G.; Zhe, B.; Lingbo, F.; Baodeng, H. The Effect of Precipitation on Hydropower Generation Capacity: A Perspective of Climate Change. *Front. Earth Sci.* **2020**, *8*, 268. [CrossRef]
3. United Nations: Climate Action. Available online: <https://www.un.org/en/climatechange/what-is-renewable-energy> (accessed on 5 June 2022).
4. Africa Energy Review 2021. Available online: <https://www.pwc.com/ng/en/assets/pdf/africa-energy-review-2021.pdf> (accessed on 5 February 2022).
5. UNIDO & ICSHP World Small Hydropower Development Report 2013. Available online: [https://www.unido.org/sites/default/files/files/2020-08/WSHPDR\\_2013\\_Final\\_Report\\_1.pdf](https://www.unido.org/sites/default/files/files/2020-08/WSHPDR_2013_Final_Report_1.pdf) (accessed on 3 May 2022).
6. Rwanda Energy Group. Power Plants. Available online: <http://www.reg.rw/what-we-do/generation/power-plant> (accessed on 2 February 2022).
7. Gasore, A.; Ahlborg, H.; Ntagwirumugara, E.; Zimmerle, D. Progress for on-grid renewable energy systems: Identification of sustainability factors for small-scale hydropower in Rwanda. *Energies* **2021**, *14*, 4. [CrossRef]
8. REMA: Climate Change and Natural Disasters. Available online: <https://www.rema.gov.rw/soe/chp9.php#:~:text=The%20rainfall%20patterns%20are%20characterized,one%20from%20June%20to%20August> (accessed on 25 August 2022).
9. Jahandideh-Tehrani, M.; Zhang, H.; Helfer, F.; Yu, Y. Review of climate change impacts on predicted river streamflow in tropical rivers. *Environ. Monit. Assess.* **2019**, *191*, 12. [CrossRef] [PubMed]
10. Rwanda Ministry of Lands, Environment, Water and Mines. National Adaptation Programmes of Action to Climate Change, NAPA-Rwanda 2006. Available online: <https://unfccc.int/resource/docs/napa/rwa01e.pdf> (accessed on 4 April 2022).
11. IRENA, Renewable Power Generation Costs 2020. Available online: [https://www.irena.org/-/media/Files/IRENA/Agency/Publication/2018/Jan/IRENA\\_2017\\_Power\\_Costs\\_2018.pdf](https://www.irena.org/-/media/Files/IRENA/Agency/Publication/2018/Jan/IRENA_2017_Power_Costs_2018.pdf) (accessed on 7 May 2022).
12. Colorado Energy Office. The Small Hydropower Handbook. Available online: <https://extension.colostate.edu/docs/energy/hydro-handbook.pdf> (accessed on 8 May 2022).
13. Moshfegh, B. World Renewable Energy Congress 2011. Linköping-Sweden. Available online: <https://ep.liu.se/ecp/057/ecp57.pdf> (accessed on 3 June 2022).
14. Uhumwangho, R.; Odje, M.; Okedu, K.E. Comparative analysis of mini hydro turbines for Bumaji Stream, Boki, Cross River State, Nigeria. *Sustain. Energy Technol. Assess.* **2018**, *27*, 102–108. [CrossRef]
15. Abd Hamid, M.F.; Ramli, N.A.; Napiah, S.N.B.M. Factors Affecting Mini Hydro Power Production Efficiency: A case study in Malaysia. In Proceedings of the 2017 3rd International Conference on Power Generation Systems and Renewable Energy Technologies (PGSRET), Johor Bahru, Malaysia, 4–6 April 2017.
16. Singh, K.; Singal, S.K. Operation of hydro power plants—a review. *Renewable. Sustain. Energy Rev.* **2017**, *69*, 610–619. [CrossRef]
17. Aggidis, G.A.; Luchinskaya, E.; Rothschild, R.; Howard, D.C. The costs of small-scale hydro power production: Impact on the development of existing potential. *Renew. Energy* **2010**, *35*, 12, 2632–2638. [CrossRef]
18. Papapetrou, M.; Kosmadakis, G. Levelized Cost of Electricity Resource, environmental, and economic aspects of SGHE. 2022. Available online: <https://www.sciencedirect.com/topics/engineering/levelized-cost-of-electricity> (accessed on 29 October 2022).
19. Patro, E.R.; Kishore, T.S.; Haghighi, A.T. Levelized Cost of Electricity Generation by Small Hydropower Projects under Clean Development Mechanism in India. *Energies* **2022**, *15*, 4. [CrossRef]
20. Branker, K.; Pathak, M.J.M.; Pearce, J.M. A review of solar PV levelized cost of electricity. *Renew. Sustain. Energy Rev.* **2011**, *15*, 9, 4470–4482. [CrossRef]
21. Ouyang, X.; Lin, B. Levelized cost of electricity (LCOE) of renewable energies and required subsidies in China. *Energy Policy* **2014**, *70*, 64–73, 2014. [CrossRef]
22. Nasution, M.A.; Ambarita, H.; Siregar, I. Social and technical barriers that affect the growth of small-scale hydropower independent power producers in Indonesia. *IOP Conf. Ser. Mater. Sci. Eng.* **2018**, *420*, 1. [CrossRef]
23. Bernardes, J., Jr.; Santos, M.; Abreu, T.; Prado, L., Jr.; Miranda, D.; Julio, R.; Viana, P.; Fonseca, M.; Bortoni, E.; Bastos, G.S. Hydropower Operation Optimization Using Machine Learning: A Systematic Review. *AI* **2022**, *3*, 78–99. [CrossRef]
24. Falchetta, G.; Kasamba, C.; Parkinson, S.C. Monitoring hydropower reliability in Malawi with satellite data and machine learning. *Environ. Res. Lett.* **2020**, *15*, 1. [CrossRef]
25. Jung, J.; Han, H.; Kim, K.; Kim, H.S. Machine learning-based small hydropower potential prediction under climate change. *Energies* **2021**, *14*, 12. [CrossRef]

26. Sapitang, M.; Ridwan, W.M.; Kushiari, K.F.; Ahmed, A.N.; El-Shafie, A. Machine learning application in reservoir water level forecasting for sustainable hydropower generation strategy. *Sustainability* **2020**, *12*, 15. [CrossRef]
27. Kumar, K.; Saini, R.P. Application of machine learning for hydropower plant silt data analysis. *Mater. Today Proc.* **2021**, *46*, 5575–5579. [CrossRef]
28. Yang, S.; Wei, H.; Zhang, L.; Qin, S. Daily power generation forecasting method for a group of small hydropower stations considering the spatial and temporal distribution of precipitation—South China case study. *Energies* **2021**, *14*, 15. [CrossRef]
29. Bordin, C.; Skjelbred, H.I.; Kong, J.; Yang, Z. Machine learning for hydropower scheduling: State of the art and future research directions. *Procedia Comput. Sci.* **2020**, *176*, 1659–1668. [CrossRef]
30. Andrei, N. Scaled conjugate gradient algorithms for unconstrained optimization. *J. Comput. Optim. Appl.* **2007**, *38*, 401–416. [CrossRef]
31. Møller, M.F. A scaled conjugate gradient algorithm for fast supervised learning. *Neural Netw.* **1993**, *6*, 525–533. [CrossRef]
32. U.S. Geological Survey. Estimating Basin Lagtime and Hydrograph-Timing Indexes Used to Characterize Stormflows for Runoff-Quality Analysis. Available online: [https://pubs.usgs.gov/sir/2012/5110/pdf/sir2012-5110\\_text.pdf](https://pubs.usgs.gov/sir/2012/5110/pdf/sir2012-5110_text.pdf) (accessed on 5 February 2022).
33. The British Hydropower Association A GUIDE TO UK MINI-HYDRO. Available online: <https://www.british-hydro.org/wp-content/uploads/2018/03/A-Guide-to-UK-mini-hydro-development-v3.pdf> (accessed on 4 February 2022).
34. IRENA. Renewable Energy Technologies: Cost Analysis Series. 1, Power sector 3/5. Available online: [https://www.irena.org/-/media/Files/IRENA/Agency/Publication/2012/RE\\_Technologies\\_Cost\\_Analysis-HYDROPOWER.pdf](https://www.irena.org/-/media/Files/IRENA/Agency/Publication/2012/RE_Technologies_Cost_Analysis-HYDROPOWER.pdf) (accessed on 5 November 2022).
35. Zamfir, M.; Manea, M.D.; Ionescu, L. Return on Investment—Indicator for Measuring the Profitability of Invested Capital. *Valahian J. Econ. Stud.* **2016**, *7*, 79–86. [CrossRef]

**Disclaimer/Publisher’s Note:** The statements, opinions and data contained in all publications are solely those of the individual author(s) and contributor(s) and not of MDPI and/or the editor(s). MDPI and/or the editor(s) disclaim responsibility for any injury to people or property resulting from any ideas, methods, instructions or products referred to in the content.